1126 *KSME International Journal, Vol. 12, No. 6, pp. 1126~1134, 1998*

A Study on the Thermal Behavior in Microaccelerometer Manufacturing Processes

Ok Sam Kim*

(*Received March 3, 1998*)

Single crystal silicon(SCS) is used in a variety of microsensor applications in which stresses and other mechanical effects may dominate device performance. One of major problems associated with the manufacturing processes of the microaccelerometer based on the tunneling current concept is temperature gradient and thermal stressess. This paper deals with finite element analyses of residual stresses causing popping up, which are induced in micromachining processes of a microaccelerometer. The authors model temperature-dependent mechanical properties during focused ion beam(FIB) cutting and Pt deposition processes. The maximum thermal strain of 0.0012 occurred at the readout gap of the microaccelerometer during the Pt deposition process. The stress produced during the heating process of FIB cut was also found to be about 33~36 MPa and cooling process the maximum equivalent stress of about 34MPa still at the right corner of readout gap. The calculated maximum displacement occurred at the readout gap was 0.14 μm. This is still smaller than the popping up of about 2 μm observed in the experiment. The reason for this popping up phenomenon in munufacturing processes of microaccelerometer may be the bending of the whole wafer or it may come from the way the underetch occurs. Different SOI material and a new geometry of the accelerometer are under investigation. We want to seek after the real cause of this pop up phenomenon and diminish this by changing munufacturing processes of microaccelerometer.

Key Words: Thermal Behaviors, Finite Element Method, Microaccelerometer, SOI wafer, Residual Stress and Deformation, Popping Up.

1. Introduction

In the past decade, much attention has focused on single crystal silicon(SCS) micromechanical structures. The potential for merging these structures with integrated circuits to create microelectromechanical systems(MEMS) has been a major driving force behind the research(Bryzek, 1996). MEMS researches combine the advantage of small size and excellent mechanical properties of SCS with low cost according to batch manufacturability(Cho 1993; Kim, 1993). Presently microfabricated acceleration sensors have become of growing importance, and some sensors are already commercially available. Recently, there has been growing interest in micromachined silicon accelerometers for applications to automotive equipment systems such as airbag, anti-lock braking system(ABS), active suspension and navigation instrumentation(Moore, et al., 1995). Among them, airbag accelerometers open the most immediate and the largest market, whose demand for high reliability, mass production and high sensitivity to both velocity change and vibration cannot be met easily by conventional electromechanical sensor technology. For airbag applications, SCS accelerometers show a strong potential due to simple detection circuit and moderate performance characteristics.

Over the past four or five years, numerical modeling of microsensors and microstructures has gradually been developed as a field of MEMS

* Dept. of Mechanical Engineering, Yosu National University Cheonnam, 550-749, Korea.

design process (Lee, et al., 1982; Nabors, et al., 1992; Senturia, et al., 1993; Crary, et al., 1991). The advantage of numerical analyses for prediction of device performance as well as device limitations has been verified in many problems (Pourahmadi, et al., 1990). In the design of microsensors and microstructures, a multitude of layers such as thermal oxide and coating are grown and deposited at different processes to achieve certain mechanical and/or electrical geometries and functions. Due to different mechanical and physical properties of these layers, the device usually experiences various thermal and mechanical loading resulting in displacements and residual stresses which are often not easy to predict by experimental approaches (Richard, 1993). Successful analysis and design of the microaccelerometer based on the tunneling current concept using silicon on insulator (SOI) wafer depend on the knowledge about normal mechanical properties of the SCS layer such as yield stress, Young's modulus and Poisson's ratio, and their control through manufacturing process. However, these computer simulations seem essential for microaccelerometer analysis and design, since it is often very difficult to precisely measure physical/mechanical properties in a micro and nanoscopic world (Johansson, et al., 1989; Yang et al., 1996; Resnick, et al., 1994; Pisano, et al., 1990; Cho, et al., 1994; Cho, et al., 1994).

In this paper, we study some of the micromachining processes of SCS for the microaccelerometer, and their subsequent processes which might affect thermal and mechanical loads. The finite element method (FEM) has been a standard numerical modeling technique extensively utilized in structural engineering discipline for computer design of microaccelerometer. We are developing a high-senstitive microaccelerometer based on a tunneling current concept through an international collaborative project for microaccelerometer undesirable deformation, i. e. popping up occurred. We want to know the real cause of this phenomenon and diminish this by changing manufacturing processes of microaccelerometer.

2. Fabrication and Modeling of Microaccelerometer

In the fabrication of the microaccelerometer, SOI wafer is used as a starting material.

SOI wafer is promising since the top layer silicon is SCS and no assembly after the processing is necessary. Only one lithographic step and simple wet etching are required to create microstructure. Single crystal silicon may be used to make complex micromechanical components. Batch fabrication of these parts promises outstanding dimensional control, which will facilitate assembly. Unfortunately, since silicon is a brittle material, silicon mechancal devices and parts are not yet abundant. If silicon is to be widely used in commercial applications its reliability and mechanical robustness must be established. SOI wafer produced through fusion bonding and etching is used in a variety of microaccelerometers in which stresses and other mechanical effects could dominate device behaviors. The capacitive microaccelerometer based on a tunneling current cencept has the potential of high performance, although it requires slightly complex signal-processing circuit for servo-system and fabrication steps such as anodic bonding to realize a narrow gap for a sensing capacitor (Kim, et al., 1997).

The manufacturing process of SOI wafer consists of (1) growing a thermal oxide SiO_2 layer (2 μm) on a main substrate (500μm) and a SiO_2 layer (2μm) on a handle substrate (SCS) of paddle, (2) bonding a handle substrate to a main substrate during 2hr. The bonding is achieved by attaching the oxidized surfaced of the two substrates each other with pressure, and by inserting them into an oxidizing atmosphere at about 1000 ~ 1100℃. Typically, the substrates are pressed together to expel most of air, bubble and void in between the bonded surfaces. The handle substrate is then thinned to some extent using micro grinding and chemical micro polishing (CMP) at room temperature.

Figure 1 shows a perspective of the microaccelerometer based on the tunneling current con-

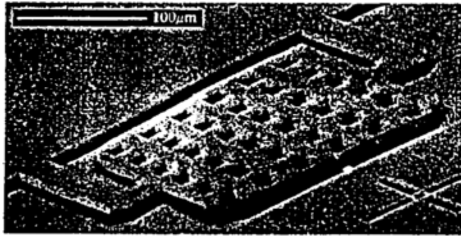

(a) SEM image for vibrating trial product of microaccelerometer.

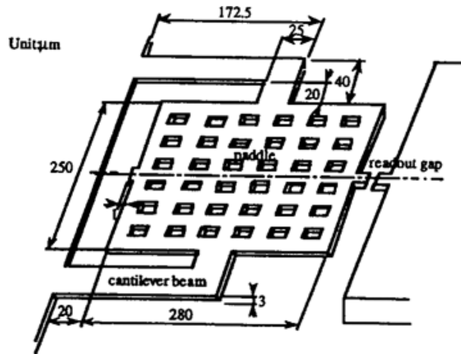

(b) Rough configuration.

Fig. 1 Schematic view of microaccelerometer.

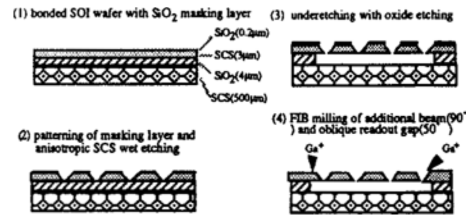

(a) Fabrication steps for the microaccelerometer

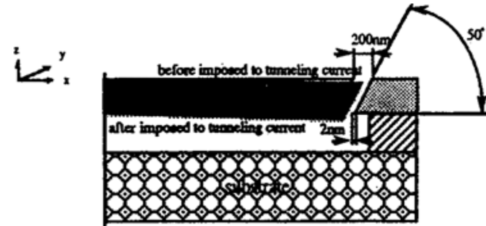

(b) Operating principles according to a tunneling current concept

Fig. 2 Fabrication steps and operating principles of the microaccelerometer.

cept, where a simple cantilever beam, paddle and supporting rims are micromachined from a SOI wafer {100} face. SOI wafer is promising since the top layer (thickness 3μm) silicon is single crystalline and no assembly after the processing is necessary. The paddle of the microaccelerometer is designed symmetric with respect to the direction of the beam. The paddle of microaccelerometer having a lot of holes due to etching has the following two roles, i. e. (1) carrying an extra proof mass to enhance inertia force, and (2) producing electrostatic force as a part of condensor to control position as shown in Fig. 1 (b).

The fabrication steps for the microaccelerometer which are shown in Fig. 2 (a) can be summarized as follows : (1) oxidation of the SOI wafer to create a masking layer (0.2μm), (2) anisotropic wet etching of the top Si layer of 3μm thickness with KOH, (3) wet etching in HF (conc.) to undercut the paddle(4μm) with silicon oxide (SiO_2) layer, and (4) FIB cut to mill the readout gap and to fully release the paddle. The readout gap is machined to have a gap width of 200nm by the focused ion beam(FIB) technology. The paddle is pulled to have the gap width of about 2μm, which almost allows the flow of tunnel current as shown in Fig. 2 (b). When z-direction acceleration is applied to the substrate, the readout gap tends to be narrower, and then the tunneling current flows. To do so, electrical voltage is applied to the paddle and substrate, and the paddle is pulled by the electrostatic force. The applied voltage must be less than 15 V, considering its supply resource. The change of applied acceleration is converted from the compensation voltage. Compensation voltage for the acceleration change should be about 0. 3 V. The deposition of an appropriate metal layer(Pt) will be necessary as a final step to assure good contact surface in the readout gap.

Now the SOI wafer utilized has the problem that the paddle of microaccelerometer is popping up (max. 2 μm at the readout gap) after FIB cut as shown in Fig. 3. The reason for this popping up in paddle may be the deformation according to some residual stress caused during the whole producing process mentioned above. The mechanical properties of SCS and SiO_2 are very important because the microaccelerometer is

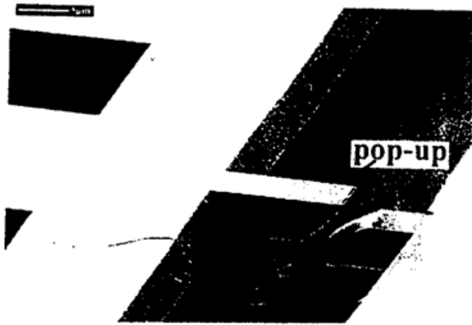

Fig. 3 Paddle popping up after FIB cut.

Table 1 Mechanical properties of SCS {100} face.

Properties	Value	Unit
Young's modulus	134.2	GPa
Poisson's ratio	0.064~0.279	
Shear modulus	50	GPa
Fracture toughness	0.95	$MPam^{1/2}$
Yield strength	6.8~7.1	GPa
Bulk modulus	91.9	GPa
Thermal line expansion	2.6~4.7	μK^{-1}

basically constructed on SOI wafer by the micro and nano technology of silicon. The behaviors and properties of SOI wafer as an electronic material are well known, but its isotropic and anisotropic mechanical properties are less so.

Table 1 presents a list of mechanical characteristics of SCS {100} face. Although SCS is a brittle material, it is not as fragile as is often believed. One of the primary reasons for studying thermal behavior in microaccelerometer manufacturing processes is because temperature gradients may induce stress in the paddle. When this stress exceeds the yield strength of the paddle, deformation and fracture would occur.

Algorithms of computational procedures for elasto-plastic residual stress occurred in SOI wafer and microaccelerometer manufacturing process are unconditionally stable and accurate for moderate strain increments as shown in Fig. 4. The authors seek for the general structure of the governing equation from cases 1 and 2. Let then

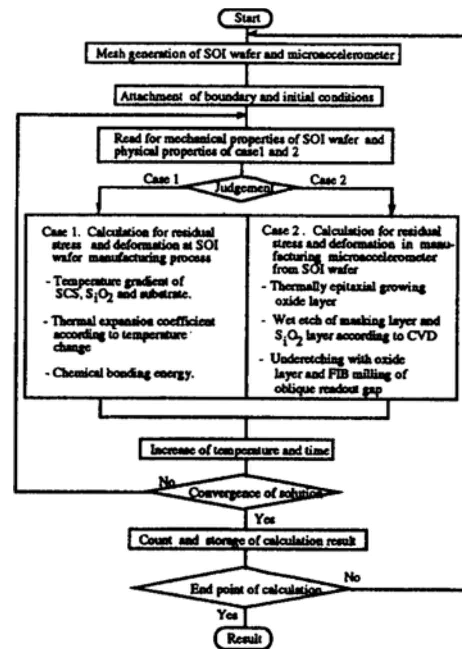

Fig. 4 Analysis flow for residual stress and deformation of SOI wafer and microaccelerometer.

assume the system under consideration can be separated into two independent thermal stress and deformation subsystems. Stress calculations also assume that the vertical temperature gradient in the microaccelerometer can be ignored. In case 1, the thermal stress is caused due to the temperature gradient of SCS, SiO_2 and substrates with different thermal expansion coefficients. This is not discussed in this paper. In case 2, the authors consider the thermally epitaxial grown layer of oxide, the underetching of SiO_2 and the FIB milling of additional beam (90°) and oblique readout gap (50°), refferring to Table 2.

The analytical approach to microsensors is only possible for simple structures. More complex shapes involing beams or multiple layer elements are best handled by finite element techniques. The paddle part is 280μm long, 250μm wide and 3 μm thick. In the analysis the microaccelerometer volume is divided into 143 rectangular (8-node) elements. Analysis of this microaccelerometer using MARC K6.1 code, generates heat transfers and thermal stresses in a transient state (Kim, et al., 1997).

Table 2 Cyclic thermal loadings during micromachining processes.

Process	Temperature (℃)	Duration (sec.)	Appliance	Working area	Note
Isotropic wet etching	25	about 1.3	HF	Masking layer	Not considered
Anisotropic wet etching	60	about 2.5	KOH	Silicon oxide layer	Not considered
FIB cutting	80	2.0	FIB	Additional beam	Considered
FIB cutting	100	54	FIB	Readout gap	Considered
Pt deposition	400	about 120	CVD	Readout gap	Considered

Calculated temperature values at integration point are used in the thermal stress analysis to general thermal load. The history definition allows an automatic application of temperature increments based on a set of temperature values defined throughout the mesh as a function of time. Equivalent nodal forces are calculated from thermal strain increment, and then added to the nodal force vector for the solution of the analysis. The computer program calculates the residual stress-strain relation at the mid-increment for each integration point based on an incremental strain prediction for maximum popping up range on the microaccelerometer. The mean normal method (MNM) or the radial return method (RRM) establishes the response for elasto-plastic residual stress behavior of cases 2 calculating a secant stiffiness matrix at each incremental step. If the residual stresses or displacements at a step of solution convergency of the increment satisfy the chosen tolerance, no more iteration takes place.

3. Results and Discussions

The SOI wafer used has the problem that paddle is popping up after the FIB cut. This makes the readout gap much bigger than desired, and leads to high voltages necessary to further close the gap. Accurate temperature sensing of microstructure is very difficult during a steady state, and almost impossible during transient. FE analyses of temperature gradients and mechanical properties following a micromachining method

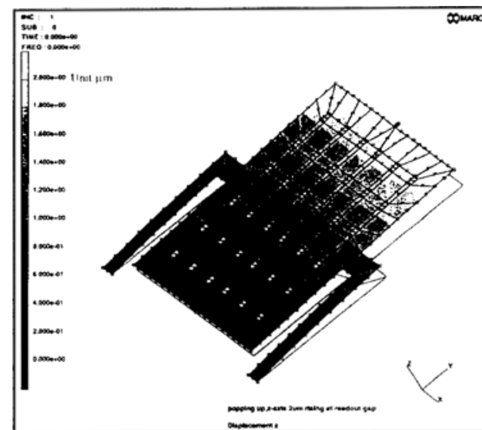

(a) Popping up, z-direction 2 μm rasing at readout gap

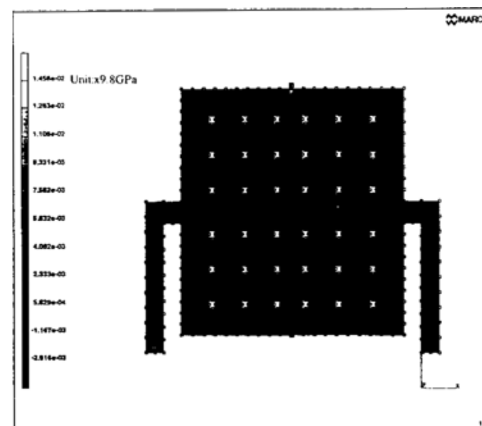

(b) Equivalent Von Mises stresses of popping up

Fig. 5 Analysis of popping up at readout gap.

for shaping SOI wafer into complex micros-

tructure, were performed for microaccelerometer based on the tunneling current concept.

In Fig. 5, contours of z-direction displacement and equivalent Von Mises stress are plotted in the case of imitating the popping up phenomenon by applying a displacement-controlled force at the readout gap. When the constraint is $2\mu m$ in the z-direction at the readout gap as shown in Fig. 5 (a), Von Mises stress is highly compressive as in Fig. 5(b). The thermal and mechanical properties of material vary with temperature, so that the temperature dependence of material properties must be taken into consideration in the stress and deformation analysis of these elements.

Figure 6(a) shows the temperature distribution of a heating process for FIB cutting(90°) at approximately heating after 4.8×10^{-9}s. Temperature rise is sufficiently low at the suspended beams. Instead, larger temperature gradient can be seen at the bottom of paddle part. The equivalent Von Mises stress of stress component is also indicated as shown in Fig. 6 (b). The magnitude of Von Mises stress is about 33~36MPa.

Figure 7 (a) shows the calculated temperature profiles of microaccelerometer at the readout gap at heating after 2.2×10^{-6}s. The distributions illustrate the contours concentration of temperature near the corner of paddle according to heat source about 100℃. Figure 7 (b) shows the z-direction displacement at the readout gap. The maximum

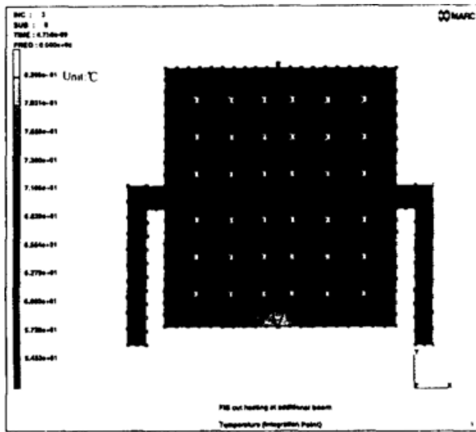

(a) Temperature distribution after 4.7×10^{-6}s

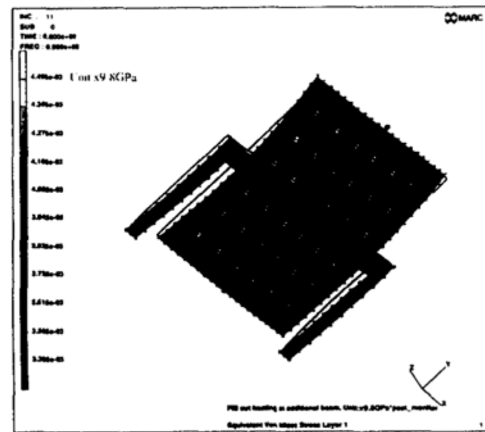

(b) Equivalent Von Mises stresses

Fig. 6 Heating process for cutting additional beam by FIB cut.

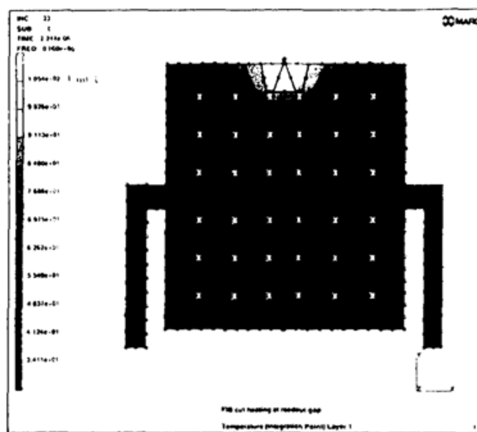

(a) Temperature distribution after 2.2×10^{-6}s

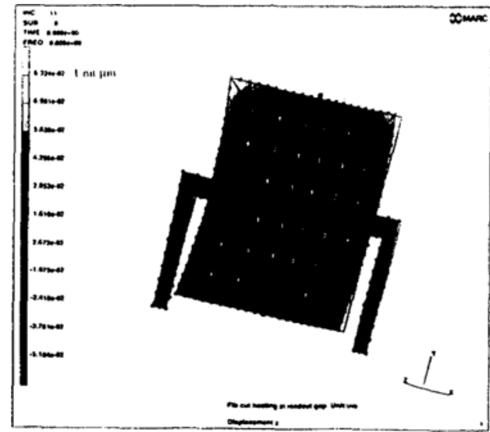

(b) Displacement

Fig. 7 Heating process for cutting readout gap by FIB cut.

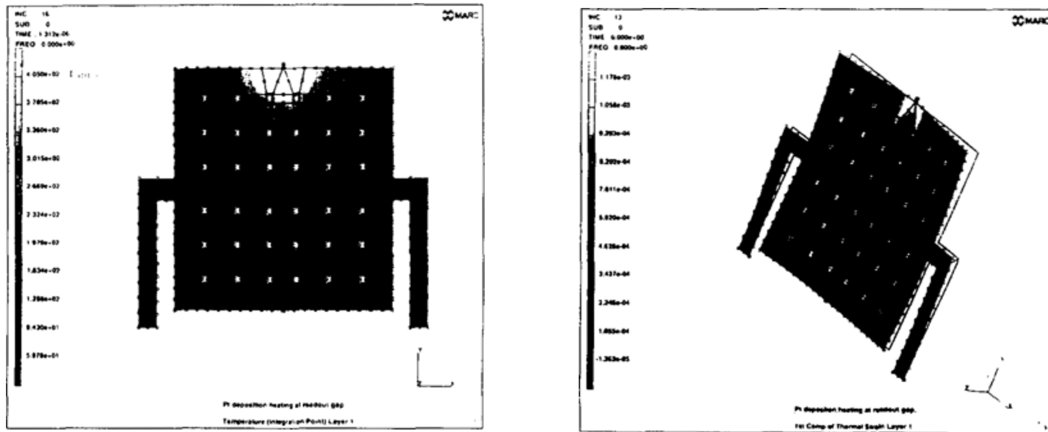

(a) Temperature distribution after 1.3×10^{-6}s (b) Thermal strain distribution

Fig. 8 Heating process for Pt deposition at readout gap.

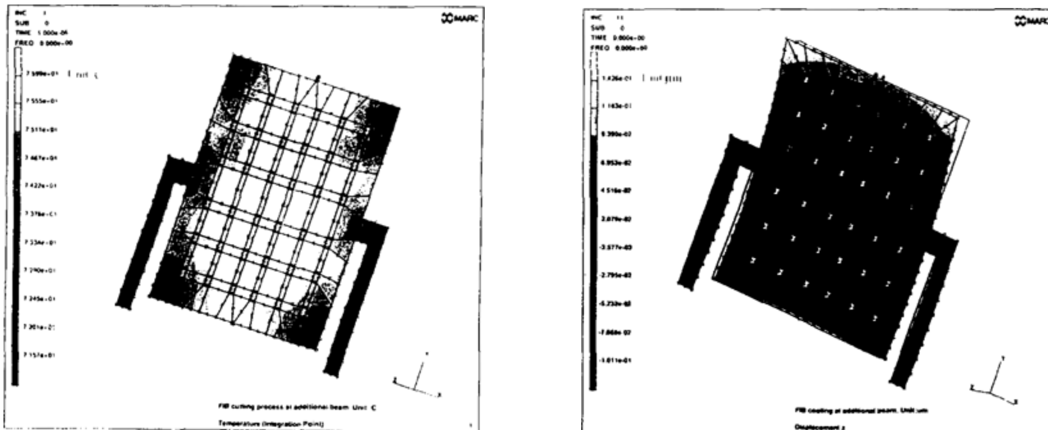

(a) Temperature distribution after 1.0×10^{-6}s (b) z-direction displacement distribution

Fig. 9 Cooling process for cutting additional beam by FIB.

displacement is 0. 083μm.

The temperature contours of Pt deposition heating process for the readout gap are depicted in Fig. 8 (a) after 1.3×10^{-6}s. The typical heating behavior curves are shown in this figure. The thermal strain at microaccelerometer is shown in Fig. 8(b). The maximum thermal strain of 0.0012 occurs at the readout gap of the microaccelerometer during the Pt deposition process.

Fiure 9 (a) shows the temperature distributions of FIB cutting(90°) process at additional beam for preventing a sticking problem. The center of paddle part becomes about 5~20℃ higher than the corner of paddle and suspended beam edges. The maximum displacement occurring at the readout gap of paddle, was found to be 0.14μm as shown in Fig. 9 (b).

Figure 10 (a) shows a calculated temperature distribution of microaccelerometer during a FIB cut cooling process after 1.1×10^{-6}s. Temperature gradients steep in the suspended beam edges and the corner of paddle. Figure 10 (b) shows calculated equivalent Von Mises stress contours of microaccelerometer for FIB readout gap cutting. The maximum equivalent stress of about 34MPa occurs at the right corner of readout gap.

Figure 11 (a) shows temperature contours representsing the cooling process of Pt deposition. Corner parts of the paddle and the suspended beams are subjected to more thermal loss due to

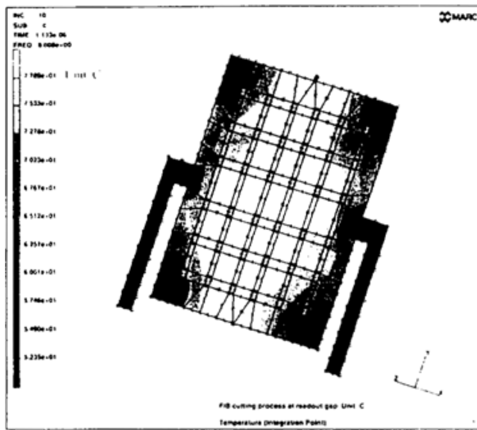

(a) Temperature distribution after 1.1×10^{-6}s

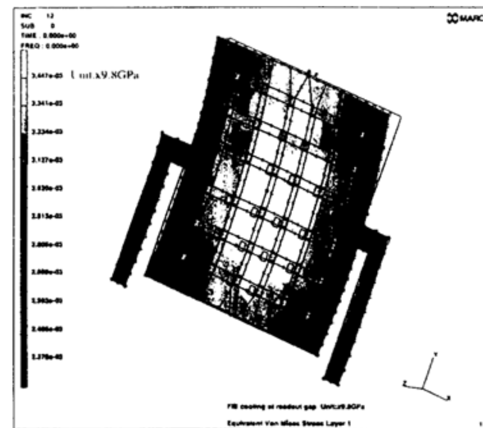

(b) Equivalent Von Mises stress distribution

Fig. 10 Cooling process for cutting readout gap by FIB cut.

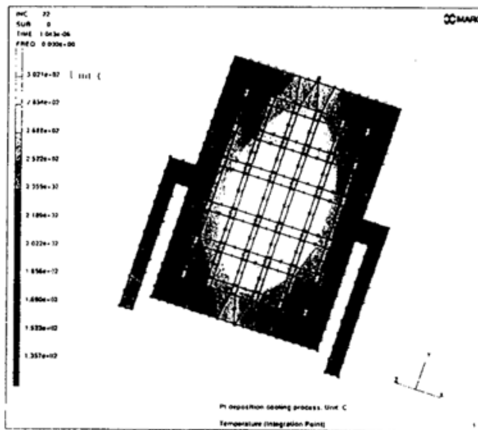

(a) Temperature distribution after 1.0×10^{-6}s

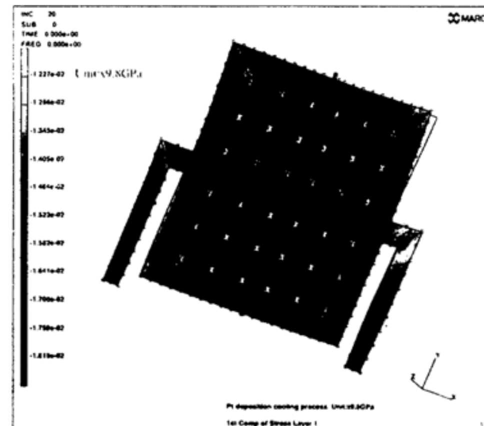

(b) Thermal stress distribution

Fig. 11 Cooling process for Pt deposition at readout gap.

their corner shape. To obtain a more uniform temperature distribution, thermal radiation should be provided to these corner parts. The thermal stress in the Pt deposition at the readout gap is illustrated in Fig. 11 (b). The compressive thermal stress distribution given in Fig. 11(b) suggests that corner parts of the paddle and the suspended beams might have larger heat transfer coefficients than the other part.

4. Conclutions

One of major problems associated with the manufacturing processes of the microaccelerometer based on the tunneling current concept is temperature gradient and thermal stressess. In this paper, we analyzed temperature and thermal stress distributions occurred in the microaccelerometer during the FIB cutting process and the Pt deposition processes. The most siginificant process was the heating and cooling process of FIB -cut of the beam. The maximum thermal strain of 0.0012 occurred at the readout gap of the microaccelerometer during the Pt deposition process. The residual stress produced during the heating process of FIB cut was also found to be about 33 ~36MPa and cooling process the maximum equivalent stress of about 34MPa still at the right corner of readout gap. The calculated maximum displacement occurred at the readout gap

was 0. 14μm. This is still smaller than the popping up of about 2 μm observed in the experiment.

The reason for this popping up phenomenon in munufacturing processes of microaccelerometer may be the bending of the whole wafer or it may come from the way the underetch occurs. Different SOI material and a new geometry of the accelerometer are under investigation. We want to seek after the real cause of this pop up phenomenon and diminish this by changing munufacturing processes of microaccelerometer. It may be necessary to simulate thermal stresses occurred in SOI wafer itself during the manufacturing process of SOI wafer.

References

Bryzek J., 1996, "Impact of MEMS Technology on Society," *Sensors and Actuators,* A56, pp. 1 ~9.

Cho, Y. H., 1993, "Micro Mechanical Engineering in Micro Electro Mechanical Systems," *Journal of the Korean Society of Mechanical Engineers,* Vol. 33, No. 6, pp. 552~570.

Cho Y. H., Kwak B. M., Pisano A. P. and Howe R. T., 1994, "Slide Film Damping in Laterally Driven Microstructures," *Sensors and Actuators,* A40, pp. 31~39

Cho Y. H., Pisano A. P. and Howe R. T., 1994, "Viscous Damping Model for Laterally Oscillating Microstruct ures," *Journal of Microelectromechanical systems,* Vol. 3 No. 2 pp. 81 ~87

Crary S., Juma O. and Zhang Y., 1991, "Software Tools for Designers of Sensor and Ac tuator CAE Systems," *IEEE Solid-state Sensor and Actuators* (Transducers 32591), San Francisco, CA, USA, pp. 498~501.

Johansson S., Ericson F. and Schweitz J., 1989, "Influence of Surface Coatings on Elasticity, Residual Stresses and Fracture Properties of Silicon Microelements," *J. Appl. Phys.,* Vol. 65 (1) Jan, pp. 122~128.

Kim, C. J., 1993, "Micromachining Technologies of MEMS," *Journal of the Korean Society of Mechanical Engineers,* Vol. 33, No. 6, pp. 499 ~514.

Kim O. S., Yoshimura S. and Yagawa G., 1997, "Analyses of Joule Heat and Stresses for Microaccelerometer Based on a Tunneling Current Concept," *JSME Centennial Grand Congress, The 10th Computational Mechanics Conference,* No. 97-7, O. S. 7-3, pp. 59~60.

Lee K. W and Wise K. D., 1982, "SENSIM : A Simulation Program for Solid-State Pressure Sensors," *IEEE Transactions on Electron Devices,* ED-29, pp. 34~41.

Nabors K., Kim S., White J. and Senturia S., 1992, "FastCap User325s Guide," *Research Laboratory of Electronics,* MIT, Cambridge, USA.

Moore D. F., Burgess S. C., Chiang H., Klaubert H., Shibaike N. and Kiriyama T., 1995, "Micromachining and Focused Ion Beam Etching of Si for Accelerometer Symposium on Micromachining and Microfabrication," *SPIE,* Vol. 2639, pp. 253~258.

Pisano A. P. and Cho Y. H., 1990, "Mechanical Design Issues in Laterally-Driven Microstructures," *Sensors and Actuators,* A21-A23 pp. 1060~1064

Pourahmadi F., Barth P., and Petersen K., 1990, "Modeling of Thermal and Mechanical Stresses in Silicon Microstructures," *Sensors and Actuators,* A21-A23, pp. 850~858

Resnick D., Cummings K., Johnson W., Chen H., Choi B. and Engelstad R., 1994, "Temperature Uniformity Across an X-ray Mask Membrane During Baking," *Journal of Vacuum Science and Technology* B, 12(6), Nov/Dec.

Richard J. Young, 1993, "Micro-Machining Using a Focused Ion Beam," *Vacuum,* Vol. 44, No. 3/4, pp. 353~360.

Senturia, S. D., et al, 1993, "Implementation of a MEMCAD System for Electrostatic and Mechanical Analysis of Complex Structures from Mask Descriptions," *Proceedings of the IEEE Micro Electro Mechanical Systems Workshop,* Fort Lauderadale, pp. 207~212.

Yang E. H. and Yang S. S. 1996, "The Quantitative Determination of the Residual Stress Profile in Oxidized p^+ Silicon film," *Sensors and Actuators,* A54, pp. 684~689